Towards the Assimilation of Near-Surface Winds from Tall Anemometric Wind Farm Towers

Joël Bédard[a], Stéphane Laroche[a,b] and Pierre Gauthier[a]

a) Department of Earth and Atmospheric Sciences, UQAM, Canada (bedard.joel@gmail.com)

b) Data Assimilation and Satellite Meteorology Section, Environment Canada, Canada

INTRODUCTION

Hourly wind power prediction plays a key role in the integration of wind power in energy production networks comprising different energy sources. The ability to predict hourly wind power up to a 48h lead time relies on accurate Numerical Weather Predictions (NWP) of near-surface winds. Although increasing the resolution of the NWP model helps to improve the forecasting skill in the lower troposphere, the main sources of forecast errors are still the analyses inaccuracy due to the limited number of near-surface wind observations assimilated, the atmospheric boundary layer modeling, and the growth of large-scale phase and amplitude errors in the analyses.

OBJECTIVES

The main objective of this project is to improve lower tropospheric analyses by assimilating near-surface wind observations from 80m anemometric wind farm towers, as well as 10m wind observations from operational surface stations in the hybrid ensemble variational data assimilation system (EnVar) developed at Environment Canada. To achieve this, it is necessary to:

1) Examine the EnVar background error covariances and evaluate near-surface flow correlation with the upper air atmosphere;
2) Develop an observation operator which includes a statistical representativeness error correction;
3) Validate the method whereby observation system experiments (OSEs) are performed using near-surface wind observations and verified against non-assimilated collocated radiosondes to assess the quality of corrections.

BACKGROUND ERROR STATISTICS

The background error statistics used in EnVar comprise a stationary homogenous component, as in a 3D-Var, and a flow dependent component from an Ensemble Kalman Filter (EnKF). The examination of the error statistics (Figure 1) shows that the vertical structures of mean variances from the stationary homogenous (NMC) and EnKF components differ near the surface where the EnKF underestimates the wind, temperature and surface pressure variances. This can be attributed to the fact that the surface analyses are currently not perturbed in the EnKF. This finding indicates that near-surface observations have a smaller impact on analyses using the EnKF statistics.

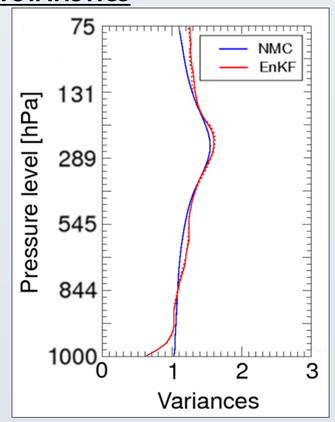

Figure 1: vertical profiles of the zonal wind variances from the NMC and EnKF methods (January 2011). For comparative purpose, the NMC error statistics are scaled by a factor of 0.6.

The evaluation of near-surface flow correlation with the upper air atmosphere reveals that the vertical structure of EnKF error correlations depends on local atmospheric stability. Indeed, Figure 2 shows that the EnKF vertical correlation length depends on the bulk Richardson number.

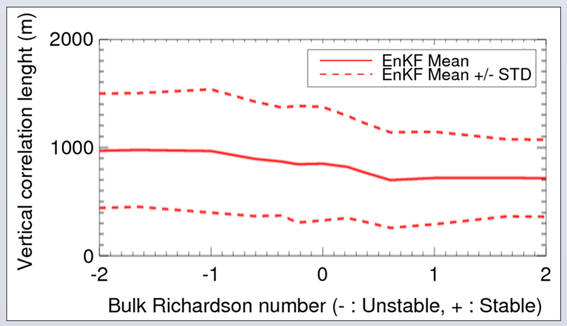

Figure 2: Vertical correlations length for zonal winds over land during July - August 2011.

This study also reveals that the EnKF background error covariances are sensitive to ensemble size. Figure 3 shows that, even when using 192 members, localization is still needed to remove spurious long-distance error correlations, especially over complex terrain.

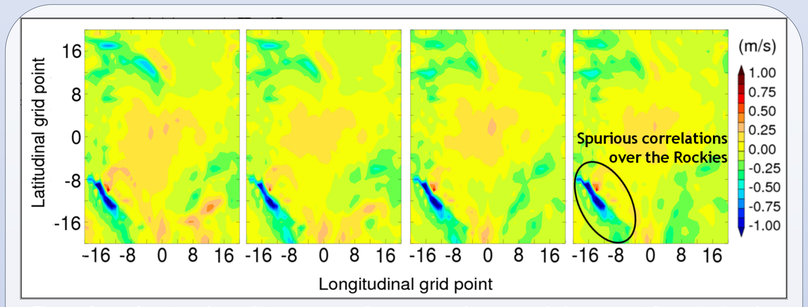

Figure 3: horizontal view of the near-surface zonal wind analysis increment for a 1m/s wind innovation during a high pressure system over Oklahoma (USA). From left to right, the panels show the results for 24, 48, 96 and 192 ensemble members.

Figure 4 (top) shows that the EnKF can capture dynamic features (e.g. coherent tilted increments associated with baroclinic structures) and the temporal correlations enable the increments to evolve with the meteorological system (not shown). The cross-correlations are also more pronounced in the EnKF error statistics (bottom) and thus, its multivariate impact for single near-surface observation is significantly higher in the vertical for all prognostic variables.

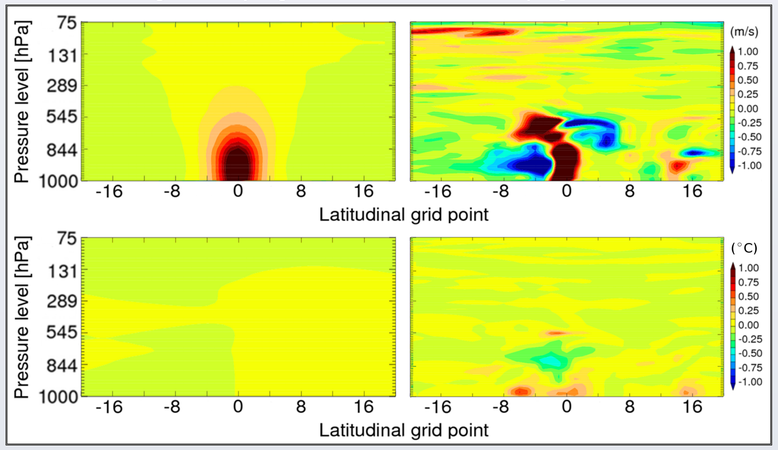

Figure 4: zonal cross section of the near-surface zonal wind (above) and temperature (below) analysis increments for a 1m/s wind innovation (low pressure system over the Atlantic Ocean). Results from NMC (left) and EnKF (right) error covariances are presented.

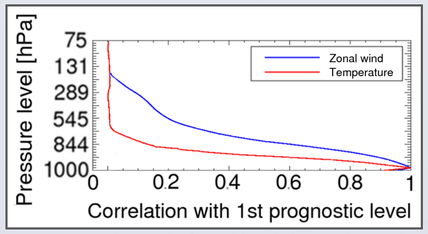

Finally, Figure 5 shows that the NMC wind correlations have a greater propagation in the vertical than temperature (EnKF covariances show similar behaviour (not shown)). This indicates that near-surface wind observations have a larger impact on analyses than near-surface temperature observations.

Figure 5: vertical profile of the NMC correlations for zonal wind and temperature.

OBSERVATION OPERATOR

To make appropriate comparisons between observations and model variables, the observation operator developed in this work involves vertical and horizontal operators: $H(x)=H_h(H_v(x))$.

1. Vertical operator

Forecast outputs are vertically interpolated to the instrument height based on Monin Obukhov similitude theory. As temperature stratification and heat fluxes at the surface have an important impact on vertical wind profiles, flow stability properties derived from predicted meteorological variables are integrated in the interpolation. As proposed by Bédard (2010), the dimensionless stability function is considered constant in height and is approximated using wind intensity forecasts (U_1 and U_2) from the model levels above (z_2) and below (z_1) the observation. The flow stability correction term for momentum (ψ) is integrated in the logarithmic vertical interpolation to estimate the anemometer level wind speed (see equations 1-3), thus replacing the usual vertical linear interpolation.

$$H(U) = \frac{u_*}{k}\left(\ln\left(\frac{z}{z_0}\right) - \Psi\right) \quad (1)$$

where

$$u_* = \frac{k(U_2 - U_1)}{\ln(z_2/z_1)}, \quad (2)$$

and

$$\Psi = \frac{(U_2 \ln(z_1/z_0) - U_1 \ln(z_2/z_0))}{(U_2 - U_1)}. \quad (3)$$

On the other hand, the wind direction is considered to vary linearly with height, as observed when analysing observations from tall wind farm towers.

2. Horizontal operator

Methods using multiple regressions can be used to reduce forecast errors as is done in model output statistics (MOS) methods. Over complex terrains where topographic features are not well resolved by the model, horizontal interpolation methods (e.g. bilinear interpolation) can be replaced by using geo-referenced weights assigned to the surrounding NWP grid points (Bédard et al., 2012). This Geophysical MOS (GMOS) is a multi-point linear regression where the horizontal interpolation is expressed as:

$$H_h(X) = \sum_i \left(A_i \cdot X_i\right) + B \quad (4)$$

where the predictors here are the zonal or meridional wind components at surrounding grid points, X_i, and A_i are the weights obtained from multiple regressions while B is a bias correction. The latter could be viewed as a static observation bias correction.

RESULTS

The forecast RMSE is decomposed into bias, amplitude (difference between forecasted and measured variability) and residual components (random errors): see equation 5. Overall from Table 1, MOS reduces the bias and slightly reduces the STD. As it is trained by minimizing the entire RMSE, MOS struggles to reduce both the amplitude and residual errors: it sometime smoothes the forecast to limit high residual errors, and thus degrades amplitude errors.

$$RMSE^2 = Bias^2 + STD^2 = Bias^2 + Amplitude^2 + Residual^2 \quad (5)$$

Training	RMSE	BIAS	STD	AMPLITUDE	RESIDUAL
Bilinear	2.42	1.04	2.08	0.81	1.90
Bilinear+MOS	1.74	0.00	1.74	0.80	1.48
GMOS(2x2)	1.65	0.00	1.65	0.69	1.45
GMOS(3x3)	1.59	0.00	1.59	0.63	1.42
GMOS(4x4)	1.56	0.00	1.56	0.59	1.41
GMOS(5x5)	1.53	0.00	1.53	0.56	1.40

Validation	RMSE	BIAS	STD	AMPLITUDE	RESIDUAL
Bilinear	2.42	1.15	2.04	0.79	1.86
Bilinear+MOS	1.76	0.32	1.73	0.84	1.46
GMOS(2x2)	1.68	0.29	1.66	0.73	1.45
GMOS(3x3)	1.64	0.25	1.62	0.67	1.44
GMOS(4x4)	1.63	0.25	1.61	0.63	1.45
GMOS(5x5)	1.63	0.25	1.60	0.61	1.46

Table 1: Zonal wind error characteristics (m/s) using different observation operators for tall anemometer towers. Left (right) panel show results using the training (validation) dataset.

On the other hand, GMOS considerably reduces the bias and both STD components (amplitude and residual errors) that can be attributed to representativeness errors. From Table 1 (left), GMOS skill increases with the number of grid-points used. However, when validating with an independent dataset (Table 1 (right)), GMOS performances saturate when using a 4x4 grid-points configuration. However, Figure 6 shows that this configuration is robust even when using a small training dataset (e.g. 1 or 2 months of data).

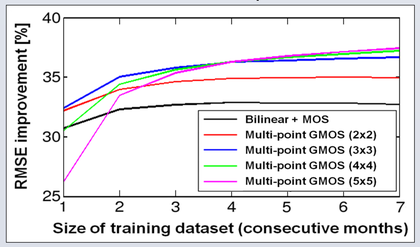

Figure 6: MOS and GMOS RMSE improvement scores (relative to Bilinear) using different configurations (from 2x2 to 5x5 grid points) as a function of the size of the training dataset.

Considering that the difference between MOS and GMOS is only the sophistication of the horizontal interpolation scheme to take into account the sub-grid scale topographic interactions with the flow, the significant performance differences between these two observation operators are essentially due to the reduction of representativeness errors by the geo-referenced statistical correction.

FUTURE WORK

In future work, the method will be validated by performing and verifying OSEs using collocated near-surface wind and radiosonde observations.